

Spherically confined H_2^+ : $^2\Sigma_g^+$ and $^2\Sigma_u^+$ states

G. Micca Longo¹, S. Longo^{1,2,3} and D. Giordano⁴

¹ CNR-IMIP, via Amendola 122/D, 70126 Bari, Italy

² Department of Chemistry, University of Bari, via Orabona 4, 70126 Bari, Italy

³ INAF-Osservatorio Astrofisico di Arcetri, Largo E. Fermi 5, I-50125 Firenze, Italy

⁴ ESA-ESTEC, Aerothermodynamics Section, Kepleerlaan 1, 2200 ag, Noordwijk, The Netherlands

E-mail: gaia.miccalongo@imip.cnr.it

E-mail: savino.longo@imip.cnr.it

E-mail: domenico.giordano@esa.int

February 2014

Abstract. The molecular ion H_2^+ is studied under strong confinement conditions produced by a spherical barrier centered in the gravity center of the molecule. Results for the potential curves are obtained by diffusion Monte Carlo methods for the ground state ($X^2\Sigma_g^+$) and the first excited state ($A^2\Sigma_u^+$), and reported as functions of the internuclear distance d for different values of the confinement radius. Results show that the compressed state corresponding to both $^2\Sigma_g^+$ and $^2\Sigma_u^+$ present deep minima in their potential curves, due to the increased space for electron wave-functions when the protons are displaced from the barrier surface.

Keywords: Confined H_2^+ , DMC, High pressures

1. Introduction

Simple confined physical systems have a very long tradition in physics [1, 2, 3, 4, 5, 6, 7], because of their importance as basic theoretical problems and as models for microscopic components of compressed matter in astrophysics (interior of stars), geophysics (giant planets), atomic and semiconductor physics (quantum dots).

In particular, confined H_2^+ , the simplest molecular system, has been the subject of many investigations as a paradigmatic model for the analysis of molecular systems under pressure: different approaches have been applied to the model of H_2^+ confinement [8, 9, 10, 11, 12, 13, 14, 15, 16].

In most previous papers, ion positions are bound to the confined surface geometry by fixed geometrical relations. Furthermore, most studies assume prolate ellipsoidal confinement: this condition is suggested by the fact that, as known, the Schrödinger equation for H_2^+ factorizes using prolate ellipsoidal coordinates. Spherical confinement was considered very sparingly [12, 17] using rather analytically heavy variational approaches. It is clear that a more straightforward approach is desirable also in view of the interest of the subject.

In this paper we apply the diffusion Monte Carlo (DMC) method to the problem of spherically confined H_2^+ . DMC is a very versatile method for such applications since an accurate value of energy can be determined using cartesian coordinates with a very natural coexistence of the different symmetries of the two-nucleus coulomb field and the spherical barrier. Details of the method can be found in a huge literature [18, 19, 20]. In the case of H_2^+ , DMC method provides an exact solution for the spherical confinement (unlike spheroidal like in previous studies), moving freely the ions inside it and strongly reducing the sphere radius, thereby raising the pressure to very high values. These possibilities are illustrated in the paper. A spherical geometry has been chosen because it is simpler and it is able to show the strong points of the DMC method. Both the ground state and the first excited state of H_2^+ are considered. Additionally, the use of theoretical concepts inspired by the DMC methodology allows to estimate some quantities and rationalize results.

We show that, contrary to intuition, H_2^+ is a stable system even into very small confining spheres. Actually, the lowest energy electronic state is a bound state with the same qualitative behavior it has in the vacuum. Even more remarkably, the repulsive excited state in the case of free ion becomes a bound one when the ion is compressed. This behavior is explained by the compression of the electronic wave function by the confining potential well.

2. Diffusion Monte Carlo

Quantum Monte Carlo (QMC) is a class of computer algorithms that are able to simulate quantum systems and to compute the electronic ground state of atoms, molecules and solids.

Diffusion Monte Carlo (DMC), in particular, is a stochastic projector method that makes use of the similarity between the imaginary-time Schrödinger equation and a generalized diffusion equation, which can be solved using a stochastic calculus and simulating a random walk. A computational code has been developed by the authors and validated as shown in the next section; no importance sampling transformation has been performed in the present paper.

When the DMC method is applied to this problem, the hamiltonian can be expressed in cartesian coordinates and there is no advantage to consider prolate spheroidal coordinates. Therefore, any confinement geometry is straightforward implemented, in particular a spherical confinement like here, and any position of nuclei is equivalent. Based on these features, in perspective, a comparison between different confinement conditions is possible, in particular to compare ellipsoidal [17] and spherical barriers.

In our simulations, the dihydrogen cation H_2^+ is placed inside an impenetrable spherical box. The two protons are considered as point sources of a Coulomb field and they are placed along the x axis at $x = \frac{d}{2}$ and $x = -\frac{d}{2}$ respectively (d being the internuclear distance). The corresponding hamiltonian (in atomic units) is:

$$\hat{H} = -\frac{1}{2}\nabla^2 + V(\mathbf{r}) + \frac{1}{d} + E_H \quad (1)$$

where E_H is the hydrogen atom energy and $V(\mathbf{r})$ is the potential energy

$$V(\mathbf{r}) = -\frac{1}{|\mathbf{r} - \mathbf{i}\frac{d}{2}|} - \frac{1}{|\mathbf{r} + \mathbf{i}\frac{d}{2}|} \quad (2)$$

The confining barrier is a sphere of radius r_0 with center in the origin of the axes. The electron is replaced by a chain of fictitious particles called walkers [18] and the Coulomb potential acts on every walker. Any walker for which $r > r_0$ (r_0 being the confinement dimension) is removed from the simulation in order to include the confinement. The confinement is realised by acting on the potential energy surface V : $V = \infty$ when $r > r_0$. By decreasing the timestep and increasing the walker number, this method, as known, converges to the exact solution of the Schrödinger equation.

During the simulation, the walkers diffuse throughout the phase space and the transition probability density for the evolution of the walkers is given by the approximate Green's function:

$$G(\mathbf{R} \leftarrow \mathbf{R}', \tau) \approx (2\pi\tau)^{-\frac{3N}{2}} \exp \left[-\frac{(\mathbf{R} - \mathbf{R}')^2}{2\tau} \right] \exp \left[-\frac{\tau(V(\mathbf{R}) - V(\mathbf{R}') - 2E_T)}{2} \right] \quad (3)$$

Every diffusion step consists of two phases: propagation and branching. At the beginning, each walker is moved from its old position \mathbf{R} to the new one \mathbf{R}' with probability

$$T = (2\pi\tau)^{-\frac{3N}{2}} \exp \left[-\frac{(\mathbf{R} - \mathbf{R}')^2}{2\tau} \right] \quad (4)$$

where τ is the time step.

The factor that determines the number of walkers surviving for next step is given by

$$P = \exp \left[-\frac{\tau(V(\mathbf{R}) - V(\mathbf{R}') - 2E_T)}{2} \right] \quad (5)$$

in which V is the potential energy and E_T is the so called energy offset that controls the total population of the walkers. When $P < 1$, the walker continues its evolution with probability P and dies with probability $1 - P$; when $P \geq 1$, the walker continues its evolution and, at the same position, a new walker is created with probability $P - 1$. From equation (5), it is clear that the walkers tend to proliferate in regions of low potential energy and to disappear in regions of high potential energy.

The energy offset E_T is determined by keeping track of changing walkers and by tuning it at every step in order to make the average walker population approximately constant [21]. A simple formula for adjusting E_T is

$$E_{T_i} = E_{T_{i-1}} + \alpha \ln \left(\frac{N_{i-1}}{N_i} \right) \quad (6)$$

where $E_{T_{i-1}}$ is the energy value at time step $i - 1$, α is a small positive parameter and N_{i-1} and N_i are respectively the number of walkers at time step $i - 1$ and the actual one.

Probabilistic method like DMC can deal with positive distributions only, so a problem arises studying an excited state wave function: the DMC algorithm is not able to maintain the fermionic symmetry of the excited state and so the solutions fall on the bosonic ground state. Nevertheless, DMC method can still be used for low excited states with distinct symmetries. The starting point is the fixed-node DMC method [19, 22, 23, 24]: a trial wave function is chosen and used to define a trial node surface that reproduces the symmetry of the excited state.

Here the $^2\Sigma_u^+$ eigenvalues are reproduced by an extra absorbing boundary placed at the centre of the box, corresponding to the yz plane.

A problem arising during computation and associated with the confinement boundary requires attention: the boundary is not truly *numerically* impenetrable and so it is possible that some walker does not see the wall and passes through it. As a matter of fact, the ensemble of walkers behaves like a kind of rarefied gas with a mean free path $\sim \sqrt{\tau}$; therefore, if the estimator is sampled after checking the barrier crossing, the effective box width is larger by a quantity of the same order. An optimization technique, based on a sub-cycling algorithm, can be applied: walkers getting closer than a few new $\sqrt{\tau}$ to the barrier can be moved with a reduced step, typically 0.1τ , for a number of cycles chosen to match the original τ . This was not found necessary to provide the plot in this work.

The DMC method can also be applied to partial confinement: outside the confining sphere, the potential energy V can be set to a large, but not infinity, value, in order to realise a penetrable confinement [15].

These last two observations provide an interesting starting point for future works.

3. Confined H_2^+

Here results for the H_2^+ electronic ground state and the first excited state are reported. About 10^3 walkers have been used in the calculation, while τ values ranged between 10^{-3} for strong confinement and the excited state and 10^{-2} for free case. The total energy (presented in eV) as a function of the internuclear separation d (presented in atomic units) is determined.

Preliminary, the calculations are validated by comparing the results for the two states with results from the literature, for the case of an unconfined ion, since no result is available for the confined system.

In Figure 1 energy eigenvalues are reported as a function of d , for the two different states of the free and mildly compressed H_2^+ . This plot is reproduced here for simpler comparison to confined states, while at the same time it provides a validation of the code used for calculations: at the scale of the plot, the curves for the free case are indistinguishable from the state of the art results.

In Figures 2 and 3 we can see the effect of different confinement dimensions. Any potential curve in these calculation ends for nuclear distance $d = 2r_0$, since it was not considered realistic to further separate away the nuclei while keeping the electron wavefunction compressed, although this calculation is formally possible.

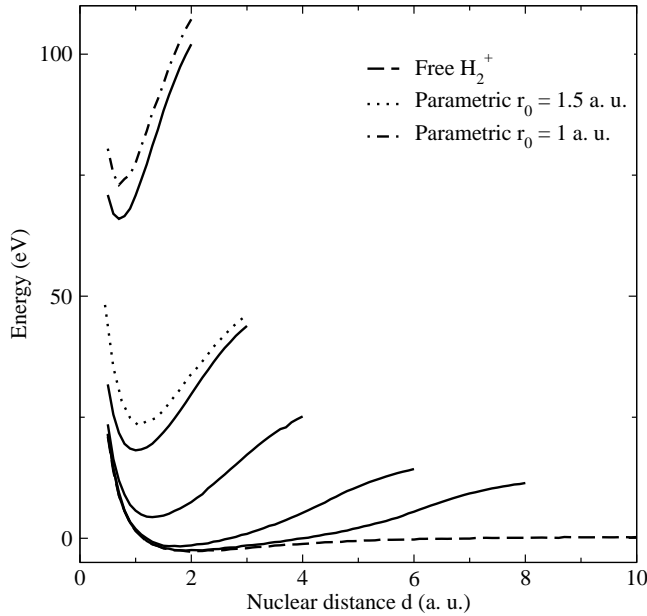
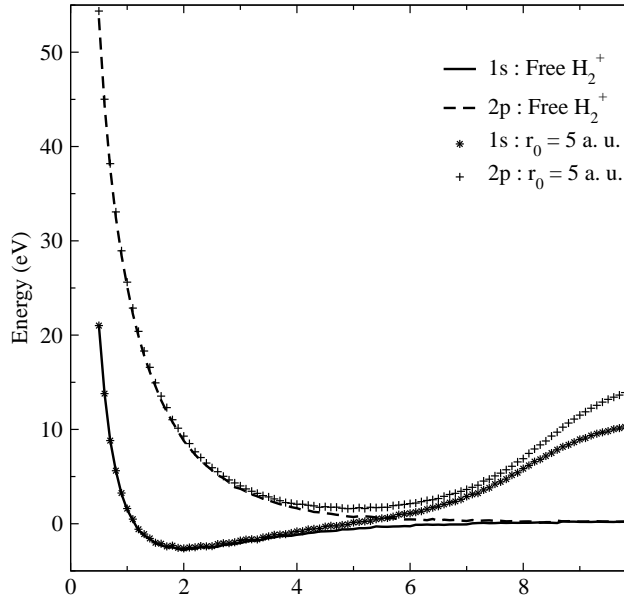


Figure 2. Free and confined H_2^+ : ground state. For better detection, note that for each r_0 the corresponding continue curve ends at $d = 2r_0$.

These curves have been normalized in order to represent the energy of the process $H^+ + H \rightarrow H_2^+(conf)$, where the atoms on the left are free. A comparison of the lowest curves in Figure 2 (for $r_0 = \infty$ and $r_0 = 4$) shows that the minimum is mostly due to a partial release of the compression energy when the nuclei are displaced from the barrier surface towards the center, leaving more effective space to the electron cloud in the Coulomb potential well of the nuclei. This interpre-

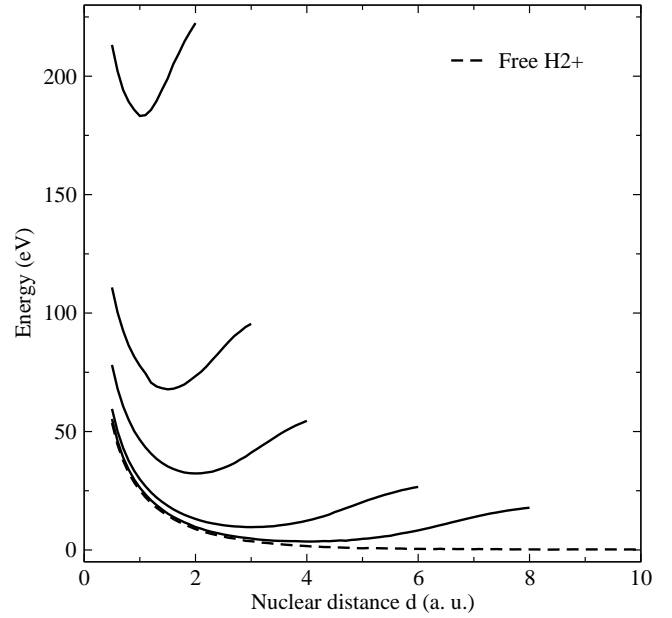


Figure 3. Free and confined H_2^+ : first excited state. For better detection, note that for each r_0 the corresponding continue curve ends at $d = 2r_0$.

tation also provides semiquantitative estimates. For example, the difference between the potential energy surface for $r_0 = 4$ at the limit value $d = 2r_0$ with respect to the corresponding value for $r_0 = \infty$ is approximately equal to the energy difference between a $2p$ and $1s$ state of the separated H atom, since the barrier at large r_0 for $d = 2r_0$ behaves like the corresponding nodal surface. This interpretation is based on the same concept used in this work to calculate excited states making use of nodal surface, therefore it will be elaborated further. For large enough confinement radius (several atomic units), the effect of the coulomb field generated by the opposite nuclei is no more relevant and, at the same time, the sphere surface in contact with the nuclei can be considered as a plane. This plane coincides with the nodal surface of the corresponding $2p_x$ orbitals in real form

$$2p_x = \frac{2p_{+1} + 2p_{-1}}{i\sqrt{2}} \propto r \exp(-r/2) \cos \theta.$$

We expect therefore to converge to the corresponding $2p$ orbital energy: this is confirmed by an independent test calculation with a single proton in the origin and a yz nodal plane. This amount to an energy difference of 10.2eV , in agreement with the DMC result. For further illustration, in 1 the potential energy surfaces for the g and u states are reported in a case of mild compression ($r_0 = 5$). It can be seen that both curves reach values close to 10.2 eV at the limit $d = 2r_0$. Calculations demonstrate the convergence of both curves to the same value 10.2 eV for larger confining spheres.

The value of the potential energy surface at the limit abscissa ($2r_0$) increases fast while increasing compression, due to the effect of pressure on the electron cloud.

When the radius of the spherical barrier is ~ 2 or lower, the expansion model cannot explain the potential energy surface features. For such strong compression, an alternative mechanism is based on the idea that, for a molecule in small containing sphere, the electron wavefunction is essentially that of the ground state of an electron in a spherical box ψ_{01} . The energy eigenvalue can then be estimated by a perturbative calculation based on such wavefunction:

$$E \sim E_{01} - \frac{2}{|\mathbf{r} - \mathbf{i}\frac{d}{2}|} >_{01} + \frac{1}{d} + E_H$$

The result for ${}^2\Sigma_g^+$ is shown on Figure 2 and it can be noticed that the mechanism accounts for the qualitative features of the potential energy surface for low values of r_0 while for a large radius, this approach is less effective and does not explain the convergence to 10.2eV .

Based on this good agreement, it is possible to use the perturbative result to discuss qualitative features of the potential energy surface. Since the kinetic energy is given by the E_{01} term which is a constant for a given r_0 , the attractive part of the potential beyond the minimum is to be attributed to the average Coulomb energy: namely the displacement of nuclei from the barrier surface allows to have higher charge density inside the nuclei potential well. The repulsive part of the potential below the minimum is essentially due to the internuclear repulsion $1/d$.

A very interesting feature emerges from Figure 3: the ${}^2\Sigma_u^+$ state, which is antibonding in the case of the free H_2^+ ion, has pronounced minimum in the case of the compressed ion. These minima have of course the same explanation as in the case of the enhanced minimum for the ground state (the previous case). This feature is interesting for astrophysical radiations transport, since it suggests that the excitation of ${}^2\Sigma_g^+$ to the ${}^2\Sigma_u^+$ state could lead to radiation diffusion and vibrational excitation of the ground state, since it cannot result in non radiative dissociation like in the case of the free ion.

For appropriate use of these results, an estimate of the corresponding pressure of the ground state is provided. This last can be calculated exactly using the relation $p = -(\partial E / \partial V)_T$, where E is the average energy per molecule and V is the volume of the confining sphere. For an estimate at $T = 0$, only the minimum of the calculated potential energy and the zero-point vibrational energy under the harmonic approximation are included. The derivative is also approximated as a finite ratio between two close curves. Under these assumptions, the zero-T pressure is \sim

$9 \times 10^5 \text{ atm}$ for mild compression $r_0 \sim 2.5$ and raises to $\sim 4.8 \times 10^7 \text{ atm}$ for more extreme compression $r_0 \sim 1.25$

4. Conclusions

This paper shows that the application of DMC method to this problem allows to obtain the energy for any position of nuclei, confinement shape, using cartesian coordinates. Energy - internuclear distance curves for the ground state (${}^2\Sigma_g^+$) and the first excited state (${}^2\Sigma_u^+$) of the H_2^+ ion under spherical confinement have been calculated for different values of the confinement radius. An appropriate nodal surface is used to select the required excited state. It is found that this molecular ion keeps a classical curve with a neat potential minimum even under conditions of very strong confinement and in spite of the very high energy of the minimum with respect to dissociation to unconfined atoms. Semiquantitative interpretation of the features of the potential energy surface are provided based on two different models for mild and strong confinement. These results support the idea that H_2^+ may be a significant constituent in hydrogen phases under very high pressure astrophysical plasmas. Furthermore, the plots reported may be used as reference in next future studies in view of the lack of alternative, easily accessible data. The technique used is versatile and may be useful to discuss similar systems even under different confinement shapes.

Acknowledgment

This research activity has been supported by the General Studies Programme of the European Space Agency through contract 4200021790 CCN2.

References

- [1] Michels A, Boer J D and Bijl A 1937 *Physica* **4** 981 – 994 ISSN 0031-8914 URL <http://www.sciencedirect.com/science/article/pii/S0031>
- [2] Groot S R D and Seldam C A T 1946 *Physica* **12** 669 – 682
- [3] Suryanarayana D and Weil J A 1976 *The Journal of Chemical Physics* **64** 510–513 URL <http://scitation.aip.org/content/aip/journal/jcp/64/2>
- [4] Yngve S 1988 *Journal of Mathematical Physics* **29** 931–936 URL <http://scitation.aip.org/content/aip/journal/jmp/29/4>
- [5] Yngve S 1986 *American Journal of Physics* **54** 1103–1106 URL <http://scitation.aip.org/content/aapt/journal/ajp/54/1>

- [6] Burrows B L and Cohen M 2006 *International Journal of Quantum Chemistry* **106** 478–484 ISSN 1097-461X URL <http://dx.doi.org/10.1002/qua.20736>
- [7] Aquino N, Campoy G and Montgomery H E 2007 *International Journal of Quantum Chemistry* **107** 1548–1558 ISSN 1097-461X URL <http://dx.doi.org/10.1002/qua.21313>
- [8] Cottrell T L 1951 *Trans. Faraday Soc.* **47**(0) 337–342 URL <http://dx.doi.org/10.1039/TF9514700337>
- [9] Singh K 1964 *Physica* **30** 211–222 ISSN 0031-8914 URL <http://www.sciencedirect.com/science/article/pii/0031891464902150>
- [10] LeyKoo E and Cruz S A 1981 *The Journal of Chemical Physics* **74** 4603–4610 URL <http://scitation.aip.org/content/aip/journal/jcp/74/8/10.1063/1.441649>
- [11] LeSar R and Herschbach D R 1981 *The Journal of Physical Chemistry* **85** 2798–2804 (Preprint <http://pubs.acs.org/doi/pdf/10.1021/j150619a020>) URL <http://pubs.acs.org/doi/abs/10.1021/j150619a020>
- [12] Gorecki J and Byers Brown W 1988 *The Journal of Chemical Physics* **89** 2138–2148 URL <http://scitation.aip.org/content/aip/journal/jcp/89/4/10.1063/1.455058>
- [13] Mateos-Corts S, Ley-Koo E and Cruz S A 2002 *International Journal of Quantum Chemistry* **86** 376–389 ISSN 1097-461X URL <http://dx.doi.org/10.1002/qua.10067>
- [14] Skouteris D, Gervasi O and Laganà A 2010 *Chemical Physics Letters* **500** 144–148
- [15] Colín-Rodríguez R, Díaz-García C and Cruz S 2011 *Journal of Physics B: Atomic, Molecular and Optical Physics* **44** 241001
- [16] Sarsa A and Le Sech C 2012 *Journal of Physics B: Atomic, Molecular and Optical Physics* **45** 205101
- [17] Burrows B L and Cohen M 2013 *Phys. Rev. A* **88**(5) 052511 URL <http://link.aps.org/doi/10.1103/PhysRevA.88.052511>
- [18] Foulkes W M C, Mitas L, Needs R J and Rajagopal G 2001 *Rev. Mod. Phys.* **73**(1) 33–83 URL <http://link.aps.org/doi/10.1103/RevModPhys.73.33>
- [19] Reynolds P J, Ceperley D M, Alder B J and Lester W A 1982 *The Journal of Chemical Physics* **77** 5593–5603 URL <http://scitation.aip.org/content/aip/journal/jcp/77/11/10.1063/1.443766>
- [20] Umrigar C J, Nightingale M P and Runge K J 1993 *The Journal of Chemical Physics* **99** 2865–2890 URL <http://scitation.aip.org/content/aip/journal/jcp/99/4/10.1063/1.465195>
- [21] Thijssen J 2007 *Computational physics* (Cambridge University Press)
- [22] Anderson J B 1975 *The Journal of Chemical Physics* **63** 1499–1503 URL <http://scitation.aip.org/content/aip/journal/jcp/63/4/>
- [23] Anderson J B 1976 *The Journal of Chemical Physics* **65** 4121–4127 URL <http://scitation.aip.org/content/aip/journal/jcp/65/10/>
- [24] Moskowitz J W, Schmidt K E, Lee M A and Kalos M H 1982 *The Journal of Chemical Physics* **77** 349–355 URL <http://scitation.aip.org/content/aip/journal/jcp/77/1/>